JOURNAL OF MATERIALS SCIENCE 7 (1972) 499-511

Study of the α to β Transformation in Boron

P. RUNOW
II. Physikalisches Institut der Universität zu Köln, Germany

The transformation of α-rhombohedral to β-rhombohedral boron was studied on a heating stage in an electron microscope. It was possible to freeze in three metastable phases. The orientation relationships of parent-, and product-phases were revealed by electron diffraction. Models were developed to explain the different transformation steps. The end-product of the transformation showed the lattice spacings of perfect β-rhombohedral boron but it was deduced that the unit cell of the transformed material had a deficiency of 9 atoms compared with the 105-atom cell of perfect β-rhombohedral boron.

1. Introduction

The largest single crystals of boron available at present are those of the β-rhombohedral polymorph ("β-boron"), on which therefore most of the previously published experimental work has been done [1-4]. The interpretation of these results is extremely difficult because of the complex structure [5, 6] of this modification. On the other hand the α-rhombohedral polymorph ("α-boron") has a relative simple structure with a well-known bonding [7]. Unfortunately the largest crystals of α-boron available at present have dimensions less than 0.2 mm [8]. Therefore only little experimental work has been done on this polymorph [2]. It is known that α-boron transforms irreversibly into β-boron at elevated temperatures [7]. Hence it seemed interesting to study the $\alpha \rightarrow \beta$ transformation and to deduce its mechanism as far as possible from the results on small crystals. If and when larger crystals of α-boron become available the limited information obtainable from small crystals should serve as a useful starting point for further studies.

The transformation was performed inside an electron microscope (Siemens Elmiskop I A) and examined by taking electron diffraction patterns and micrographs. X-ray methods could not be applied because of the smallness of the α-boron crystals and the small X-ray scattering factor of boron.

2. Experimental

The α-boron used in this study was supplied by the Institute of Inorganic Chemistry of the University of Munich. The preparation and preliminary electron microscopic examinations are described in [9].

For the heating experiments only those α-boron crystals which showed no fault contrast were used. The specimens, preferably in the form of flat needles, were placed in the Siemens heating stage on molybdenum grids where they were fixed by natural adherence. The temperature obtainable with the heating stage (about 1000° C) turned out to be insufficient to cause the transformation into β-boron and additional temperature increments were obtained by direct electron beam heating. The specimen temperature was estimated from the known beam current and focusing conditions and the calculations checked with the known melting point of silicon (see appendix). In order to obtain a uniform illumination only the defocused condenser II was used. In a second series of experiments the influence of a temperature gradient was examined by shock-heating using merely the focused condenser II.

Because the results were mainly obtained by electron diffraction, the various factors limiting the accuracy of electron diffraction measurements of lattice spacings were examined. The determination of the diffraction constant $\lambda \cdot L$ was performed by indexing the diffraction patterns of the known α-boron structure before heating. Errors caused by different specimen positions when using standards for calibration were thus

avoided. Care was taken of the effect of spikes in the reciprocal lattice and deviations between "Ewald plane" normal and beam direction. Furthermore, the variation of the diffraction constant with the azimuth angle in the photo plate, resulting from a non-compensated axial astigmatism, was taken into account. Owing to the shape of the diffraction spots, which were elongated as a result of the strain in transformed specimens, the measurement of spot distances was limited to an accuracy of 1.25%. The total error in determining unknown lattice spacings, including the calibration of the microscope, was found to be less than 2.35%.

3. Results

The results obtained from experiments with hot-stage and additional beam heating (which combination will be referred to as "furnace heating") were quite different from those with heating merely by the focused electron beam ("shock heating"). For this reason the two sets of results are discussed separately.

3.1. Results with Furnace Heating

Fig. 1 shows a diffraction pattern of monocrystalline α-boron before heating which was used for the determination of the camera constant. A furnace temperature of 1000°C and illumination with double condenser caused no change in the pattern. When, however, the defocused condenser II was used the extra spots and deformations visible in fig. 2 occurred at a beam current density of 1.7×10^{-3} A/cm^2. This corresponds to an approximate temperature of 1370°C (see appendix).

When the first extra reflections appeared, the heating was interrupted. The diffraction pattern (fig. 2), which was photographed after cooling down, shows that an irreversible change had occurred. Determination of lattice spacings from fig. 2 yields the values given in table I, where the indices were determined by comparison with d-values calculated for perfect α- or β-boron.

TABLE I d-values obtained from fig. 2 – specimen heated to 1370°C.

(hkl)	d_{hkl} (Å) (measured)	d_{hkl} (Å) (calculated from perfect structures)
$(002)^{\beta}$	4.45	4.403
$(111)^{\alpha}$	4.28	4.247
$(001)^{\alpha}$	4.04	4.066
$(222)^{\beta}$	3.97	3.968
$(220)^{\beta}$	3.85	3.708
$(110)^{\alpha}$	3.64	3.544
$(112)^{\alpha}$	2.57	2.545
$(224)^{\beta}$	2.45	2.520

It is striking that close to each α-reflection there appears a corresponding β-reflection in second order, whilst the first order is missing. The beam direction in both structures is $[1\bar{1}0]$. Except for $(111)^{\alpha}$, $(001)^{\alpha}$ and $(002)^{\beta}$ the reflections are elongated to arcs about the beam direction as the axis of rotation. This indicates bending of lattice

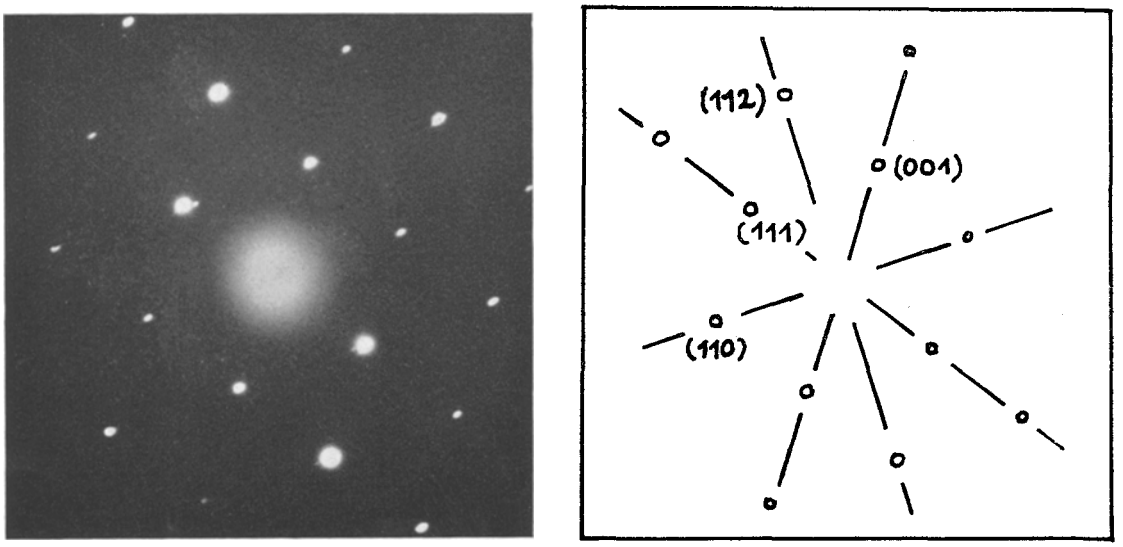

Figure 1 Diffraction pattern from monocrystalline α-boron before heating, beam direction $[1\bar{1}0]^{\alpha}$ (× 3).

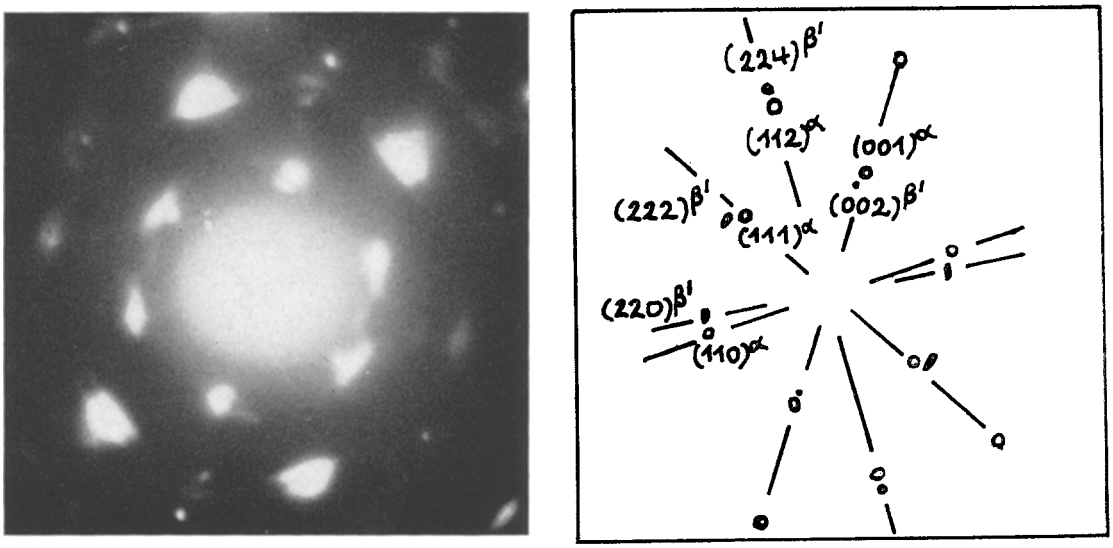

Figure 2 This diffraction pattern occurred at a specimen temperature of ≈ 1370°C, same area as in fig. 1, beam direction: $[1\bar{1}0]^{\alpha\prime\beta\prime}$.

planes belonging to the zone with axis $[1\bar{1}0]$. The diffraction pattern in fig. 2 may be imagined as the result of the super-position of a pattern from a nearly perfect α-cell and that from a β'-cell which has the same arrangement of icosahedra as the α-cell, but has a greater angle (65.45°) and half the edge length of the β-boron rhombohedron. The β'-cell may originate from the α-cell by a simple bulging out of the α-rhombohedron, because

$$a_0(\alpha) = 5.057\text{Å} \approx 1/2\, a_0(\beta) = 5.072\text{Å}$$

Therefore eight β'-cells form a unit with the dimensions of the β-boron elementary cell. The resulting rhombohedron is edge, face and body centred, when the icosahedra are regarded as large elements with the same scattering amplitude. The structure factor of this unit is:

$$F_{hkl} \begin{cases} = 0 & (hkl) \text{ mixed or all uneven} \\ \neq 0 & (hkl) \text{ all even} \end{cases}$$

Consequently the structure factor explains that only planes of β-boron with even indices appear in the diffraction pattern (fig. 2). This may be regarded as a verification for the postulated β'-cell.

Stereographic projection may be used to illustrate the orientation relation between the starting and product phases in fig. 2. Because the reciprocal lattice vectors $\vec{\mathbf{g}}_{001}{}^{\alpha}$ and $\vec{\mathbf{g}}_{001}{}^{\beta}$ form an angle near the limit of accurate measurement (≈ 1°), this deviation was neglected and $(001)^{\alpha}$ assumed to be parallel to $(001)^{\beta}$. Fig. 3a shows the orientation relationship based on fig. 2; fig. 3b that for perfect α- and β-cells having both (001) and $(1\bar{1}0)$ common.

Renewed heating of the specimen up to the temperature reached on first heating caused no further change in the diffraction pattern. This fact was characteristic of all intermediate stages occurring in the transformation process. Only an increase of the beam current (specimen temperature: ≈ 1590°C) caused a distinctive change in the periodicity of the pattern. Again the heating was interrupted. The diffraction pattern in fig. 4 was taken from the same area as in fig. 2. The measured *d*-values and indices deduced by comparison with *d*-values calculated for perfect α- and β-boron are listed in table II.

Whereas in fig. 2 $(001)^{\beta}$, $(111)^{\beta}$, $(110)^{\beta}$ and

TABLE II *d*-values obtained from fig. 4 – specimen heated to 1590°C.

(*hkl*)	d_m (Å) (measured)	d_c (Å) (calculated)	$\frac{d_m - d_c}{d_c} 100(\%)$
$(001)^{\beta}$	9.18	8.806	4.31
$(111)^{\beta}$	7.95	7.937	0.16
$(110)^{\beta}$	7.87	7.415	6.20
$(112)^{\beta}$	5.12	5.041	1.59
$(111)^{\alpha}$	4.11	4.247	− 3.23
$(001)^{\alpha}$	4.13	4.066	1.57
$(110)^{\alpha}$	3.56	3.544	0.45
$(112)^{\alpha}$	2.51	2.545	− 1.37

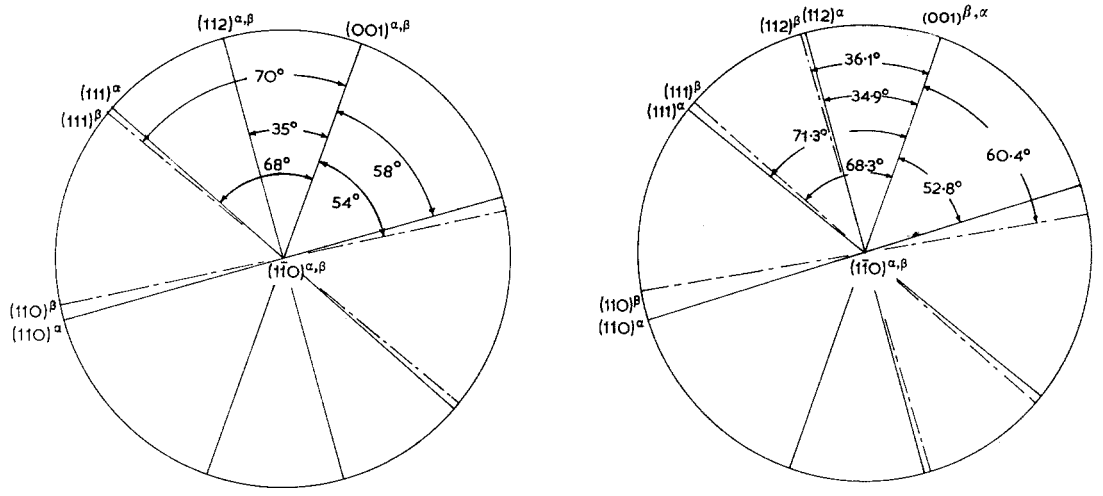

Figure 3 (a) Angles between poles from the diffraction pattern in fig. 2. (b) For perfect α- and β-cells having common (1$\bar{1}$0) and (001) planes.

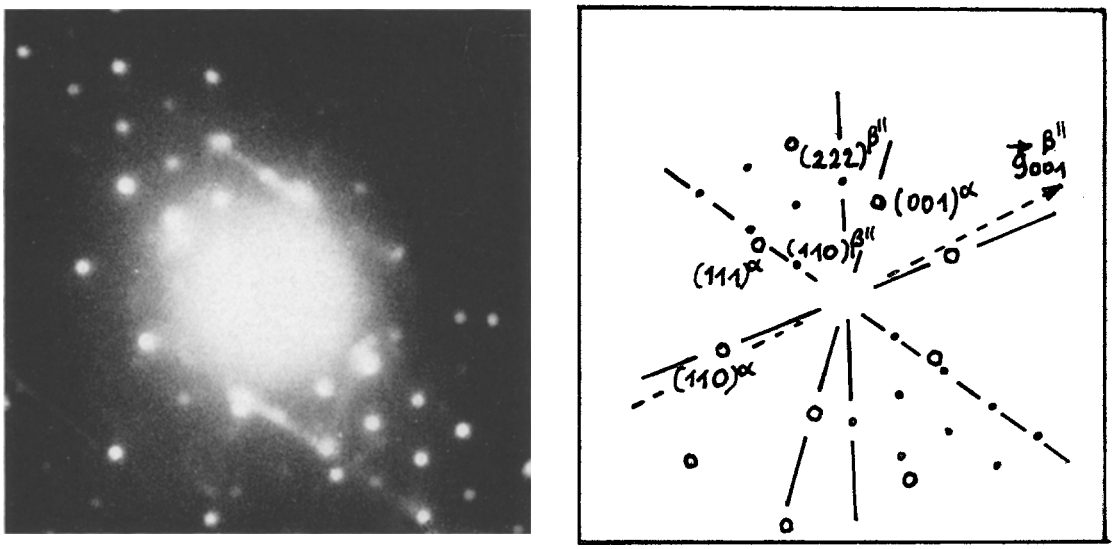

Figure 4 The α-system shows additional reflections from a β″-phase originated at ≈ 1590° C, beam direction $[1\bar{1}0]^{\alpha,\beta''}$

their odd multiples are absent, the odd orders are present in fig. 4. This indicates that the postulated rhombohedron consisting of eight β′-cells can no longer exist after heating to 1590° C. Because of the close similarity between experimentally determined *d*-values and those calculated for perfect β-boron, the product of this second transformation step will be denoted β″. With the exception of $d_m = 4.11$Å the measured *d*-values of the α-system lie within the accuracy of measurement. Probably α and β″-boron exert mutual elastic strains. This would explain the fact that the errors on $d_{001}{}^{\beta}$ and $d_{110}{}^{\beta}$ lie outside the estimated error of measurement. The decrease in $d_{111}{}^{\alpha}$, which is accompanied by an increase of $d_{110}{}^{\beta}$, looks like a misfit compensation, because both planes are parallel.

The orientation relationship of the two patterns in fig. 4 is shown in fig. 5a. It can be obtained if the β-poles in fig. 3b are rotated 48.5° clockwise about the [1$\bar{1}$0] axis keeping the α-system fixed (see fig. 5b). This rotation makes $(1\,1\,0)^{\beta}$ parallel to $(1\,1\,1)^{\alpha}$.

Renewed heating with slightly increased beam

current (specimen temperature: ≈ 1640°C) caused the α-pattern and the diffuse "streaks" seen in fig. 4 to disappear (see fig. 6). An accurate analysis shows that some of the lattice spacings seen at the β″-stage have changed markedly (see table III).

TABLE III *d*-values obtained after heating to 1640°C ("afterwards") compared with those resulting from the previous (1590°C) treatment ("before").

(*hkl*)	d_m (Å) (before)	d_m (Å) (afterwards)	d_c (Å)	$\frac{\Delta d_m}{d_c} 100(\%)$
(001)	9.18	9.23	8.806	+ 0.57
(111)	7.95	8.35	7.937	+ 5.04
(110)	7.87	7.78	7.415	− 1.21
(112)	5.12	5.32	5.041	+ 3.98

The product of this third step will be denoted β″. Continued heating for 10 min at ≈ 1640°C showed no further striking changes in the diffraction pattern but it was found that the measured lattice spacings agree within the accuracy of measurement with those calculated for perfect β-boron (see table IV).

In electron micrographs of the different transformation steps no fault contrast is clearly visible, though faults must be present in the transformed specimen without doubt. Perhaps many of them are so closely spaced that the contrast is not resolved. Occasionally diffuse striations were observed, which can be interpreted as unresolved stacking fault contrast. The

TABLE IV *d*-values obtained from a specimen heated for 10 min at 1640°C.

(*hkl*)	d_m (Å)	d_c (Å)	$\frac{d_m - d_c}{d_c} 100(\%)$
(001)	8.85	8.806	+ 0.51
(111)	8.09	7.937	+ 1.93
(110)	7.35	7.415	− 0.88
(112)	5.08	5.041	+ 0.79

monocrystalline areas transformed from α- to β-boron had dimensions up to 20 μm. In all specimens areas could be found where the growth of the β-phase was inhibited for unknown reasons.

In order to check the hitherto somewhat ambiguously assumed orientation relationship of the α- and β″-phases, diffraction patterns with different beam directions were necessary. Because the heating-stage could not be tilted, different specimens had to be used. All independently transformed areas of the same sample showed the same diffraction patterns suggesting that always the same transformation mechanism was working. The mechanism seems to be independent of the crystallographic orientation of the specimen.

The situation is especially clear if the incident beam is parallel to [1 1 1], i.e. perpendicular to the assumed axis of rotation [1 $\bar{1}$ 0], since the planes (1 $\bar{1}$ 0) must remain parallel in both phases. This case is shown in fig. 7 and table V.

It is striking that the measured value of $d_{1\bar{1}0}{}^{\beta''}$

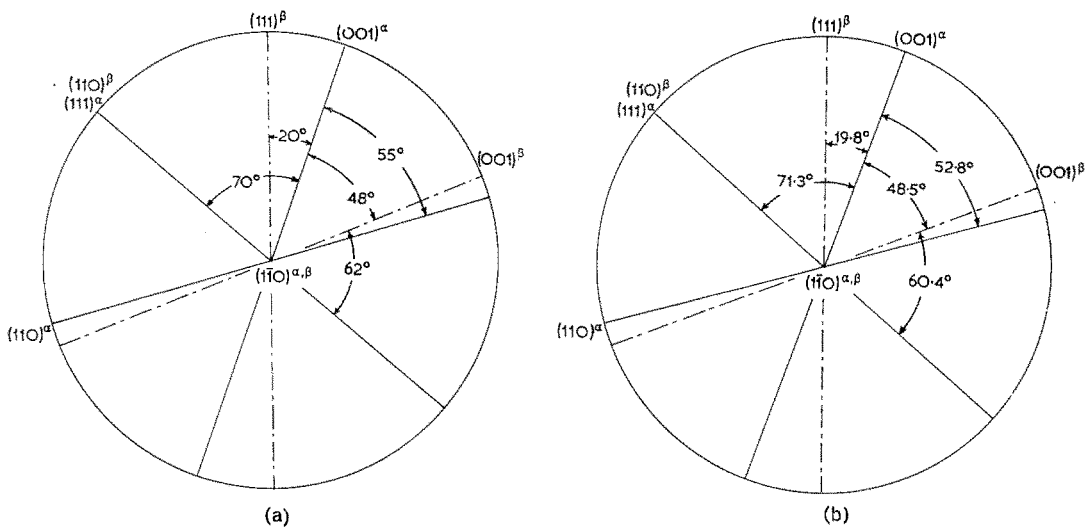

Figure 5 (a) Angles between poles from the diffraction pattern in fig. 4. (b) Orientation relationship obtained from fig. 3b by rotating the β-poles 48.5° clockwise about the [1 $\bar{1}$ 0]-axis keeping the α-system fixed.

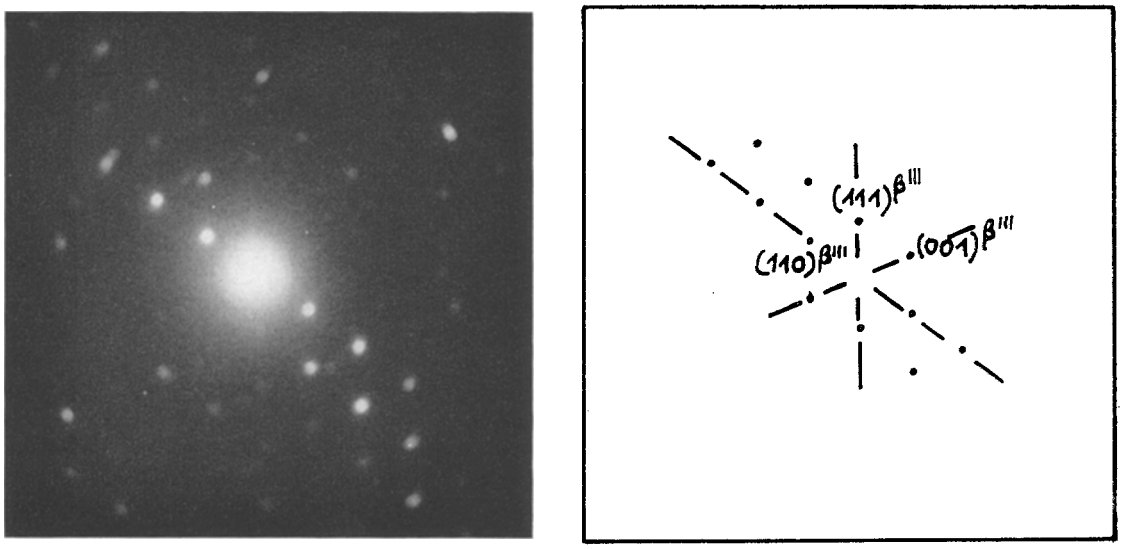

Figure 6 At a temperature of ≈ 1640°C the α-reflections have disappeared, beam direction $[1\bar{1}0]^{\beta'''}$.

TABLE V *d*-values measured and calculated for fig.7.

(*hkl*)	d_m (Å)	d_c (Å)	$\frac{d_m - d_c}{d_c} 100(\%)$
$(001)^{\beta}$	9.12	8.806	+ 3.56
$(1\bar{1}0)^{\beta}$	5.24	5.472	− 5.0
$(1\bar{1}1)^{\beta}$	4.64	4.648	− 0.17
$(1\bar{1}0)^{\alpha}$	2.62	2.479	+ 5.68

is 5.0% too small compared with the perfect β-boron whilst $d_{1\bar{1}0}{}^{\alpha}$ is 5.68% enlarged. This means that both structures take identical atomic distances along the $[1\bar{1}0]$ rotation axis by means of elastic strains. It is evident that not all planes of α-boron remain in "reflecting positions" whereas the diffraction pattern from the β″-phase shows numerous spots.

Fig. 8 shows the satisfactory agreement between calculated and measured angles (comp. fig. 7b) of α- and β″-boron planes. Additionally are marked poles which belong to a diffraction pattern with beam direction parallel to $[\bar{1}02]$ in the starting α-boron (see fig. 9).

The reproducible results from three beam directions in the starting α-boron show that the orientation relationship between α- and β″-boron may be described unambiguously by a 48.5°-rotation of the previously formed β′-cell about the common $[1\bar{1}0]$ axis.

3.2. Results with Shock Heating

With this kind of heating it was also possible to cause a transformation of primary α-boron, but the orientation relationship between starting and product phase was not reproducible, not even in different areas of the same specimen. This means that the shock heating of a small region produces a complex state of strain in the specimen which enables different transformation mechanisms to work. In specimens in which a β-phase was produced by shock heating no further noticeable grain growth was observed, because differently oriented β-grains hindered one another's growth.

It was striking that in the transformation product *d*-values were found, which exceeded those for the perfect β-boron by 3 to 6%. An unambiguous assignment was always possible (fig. 10). An idea for the interpretation of these enlarged *d*-values resulted from favourable beam directions. Assuming a pseudohexagonal unit cell, with two slightly different *a*-axes (a_1 = 10.94 Å a_2 = 11.40Å), and the *c*-axis at 24.90Å a little extended compared to perfect β-boron (cell-data of the hexagonal unit of β-boron: a = 10.94Å; c = 23.81Å), the determined *d*-values can be explained satisfactorily (see fig. 10).

4. Discussion

The present studies succeeded in freezing in and analysing different metastable products of the solid state transformation α-boron → β-boron.

It is well known that the driving force in phase transformations is the lowering of the free energy. When, however, nuclei with boundary surfaces have to be formed the consideration of geometrical correspondence leads to Ostwald's

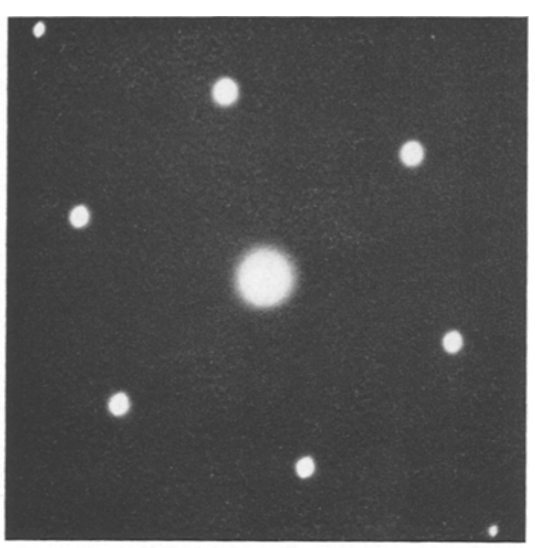

(a)

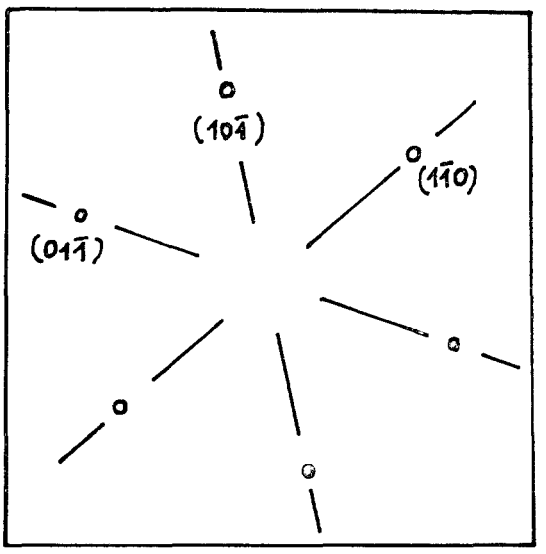

(a)

(b)

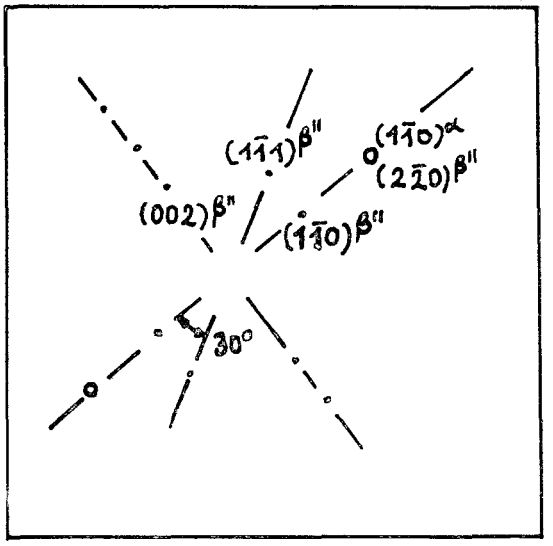

(b)

Figure 7 Diffraction pattern from the same area of the specimen (a) before heating, beam direction $[111]^{\alpha}$ (b) after formation of the β''-phase at a temperature of 1580° C.

step rule [10]. Probably this is the reason for the existence of the observed intermediate products. The interpretation of the results was difficult at the beginning because the number and range of existence of the different intermediate products were unknown.

The first transformation step ($\alpha \rightarrow \beta'$) was interpreted as a deformation of every eight α-boron units to a large unit having the cell parameters of perfect β-boron. The cell diagonal is shortened hereby, while the edge length remains approximately unaltered. Consequently the bond distances in the (1 1 1)-plane are enlarged. Fig. 11 shows lattice sites of icosahedra before and after the transformation.

As possible phase boundaries of the two modifications planes with small misfit are favoured. Calculation suggests that three lattice directions lying in (1 $\bar{1}$ 0) satisfy this condition sufficiently:

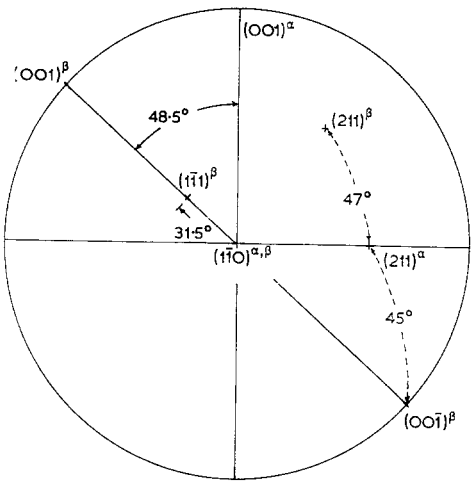

Figure 8 Stereographic projection showing the calculated angles betwen poles in α- and β″-boron after a 48.5°-rotation of the β′-cell about [1 1̄ 0].

$$\left|\begin{matrix}[001]^{\alpha}\\ [110]^{\alpha}\\ [111]^{\alpha}\end{matrix}\right| = \begin{matrix}5.057\text{Å};\\ 8.852\text{Å};\\ 12.567\text{Å};\end{matrix}\ 1/2\cdot\left|\begin{matrix}[001]^{\beta}\\ [110]^{\beta}\\ [111]^{\beta}\end{matrix}\right| = \begin{matrix}5.072\text{Å}\\ 8.541\text{Å}\\ 11.941\text{Å}\end{matrix}$$

The form of the diffraction spots (see fig. 2) and the small deviations found between measured interplanar angles and those calculated for perfect β-boron may be interpreted as a misfit compensation on a (1 1̄ 0) contact plane.

Altogether the geometrical correspondence between starting and product phase is good enough to favour this first transformation step in the sense of Ostwald's step rule. Thus the (1 1̄ 0)-plane seems to be particular and represents probably a semi-coherent phase boundary. Because of the poor fit along its normal axis the formation of plate-shaped β′-nuclei is likely.

The working transformation mechanism can be pictured as follows: because of the anisotropic bonding in the α-boron structure, the elementary cell will expand on temperature rise more in the (1 1 1)-plane containing "delta-bonds" [7] than along the edges of the rhombohedron where the bonding is covalent. Hereby the diagonal of the rhombohedron is shortened, enlarging its angle simultaneously because its edge length is maintained. Probably no essential change in the bonding structure occurs due to this deformation because a breaking of bonds would cause a rearrangement of icosahedra with more complicated movements. By this expansion the distance of icosahedra lattice sites in the (1 1 1)-plane is increased from 4.91 to 5.47Å. Assuming that the delta-bonds can continue to exist elongated by 10%, an increase of icosahedra-diameter from 3.34 to 3.74Å must take place. The average diameter of icosahedra in perfect β-boron is 3.80Å, calculated from atomic distances in an icosahedron [6].

With further temperature rise the stability in the (1 1 1)-plane gets lost, probably because the delta-bonds endure no further expansion. The unit cell rotates (preliminary description) 48.5° about [1 1̄ 0]. Hereby the planes (1 1 1) of a strained α-unit and (1 1 0) of a strained β-unit become parallel, $d_{111}{}^{\alpha}$ being 3.23% reduced and $d_{110}{}^{\beta}$ 6.20% enlarged compared with the perfect structures. Because the axis of rotation is [1 1̄ 0], the (1 1̄ 0)-planes are parallel but rotated around their normal axis in both phases. Compared with the perfect structures $d_{1\bar{1}0}{}^{\beta}$ is reduced from 5.472 to 5.24Å whilst $d_{1\bar{1}0}{}^{\alpha}$ is enlarged from 2.479 to 2.62Å. Remarkably, after the rotation, the relation $d_{2\bar{2}0}{}^{\beta} = d_{1\bar{1}0}{}^{\alpha}$ is valid. This means that a one-dimensional correspondence occurs along the axis of rotation. Planes parallel in both structures do not come into question as possible phase boundaries, because they show only poor fit.

Naturally the assumed rotation of lattice planes is only a formal description without any physical reality. An atomic mechanism was therefore derived which yields the observed orientation relationship. In fig. 12 the "+" marked icosahedra in a (1 1 0)-plane of the β′-phase move along [0 1 0] into the positions marked by "#". This may be achieved by gliding along a vector $a/2$ [0 1 0] on neighbouring (0 0 1)-planes (a = lattice parameter of the β′-cell).

Thereby the (1 1 0)-plane of β′ becomes parallel to $(1\,1\,1)^{\alpha}$ if the angle of 2° between $(1\,1\,1)^{\alpha}$ and $(1\,1\,1)^{\beta'}$, measured in the diffraction pattern of fig. 2, is neglected. Because the (0 0 1)-planes of the α- and β″-phase make an angle of 48° the assumed glide mechanism is not able to describe the observed orientation relationship. This may be attained, however, when the same glide mechanism works additionally on $(1\,1\,1)^{\alpha}$-planes along [1̄ 1̄ 2]. In order that $(0\,0\,1)^{\beta''}$ can make the measured angle of 48° with $(0\,0\,1)^{\alpha}$, the magnitude of the glide vector must increase from plane to plane by 6.97Å. This corresponds fairly well to 3/4 | [1̄ 1̄ 2] | = 7.11Å. The last-named glide mechanism also makes $(1\,\bar{1}\,0)\beta''$ parallel to $(1\,\bar{1}\,0)^{\alpha}$ as required by the diffraction pattern. Whether the two glide

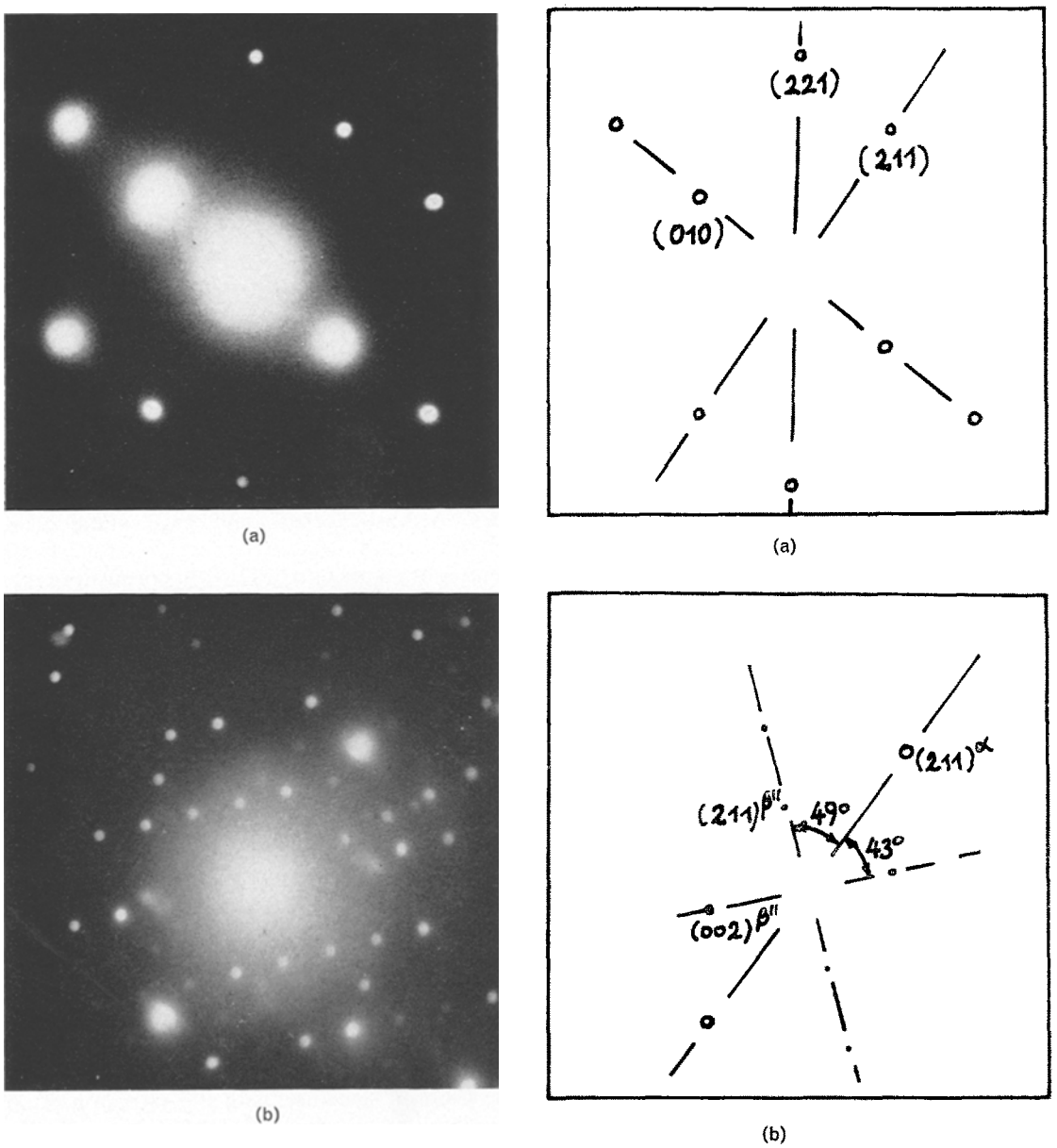

Figure 9 Diffraction pattern from the same area (a) before heating, beam direction $[\bar{1}02]^{\alpha}$ (b) after formation of β''-phase at a temperature of 1560° C.

mechanisms are really working successively is not certain. However, diffuse streaks parallel to $\vec{g}_{111}{}^{\alpha}$ and $\vec{g}_{001}{}^{\alpha}$ in the diffraction pattern (fig. 4) suggest stacking faults on these planes.

The results discussed so far show no evidence for the formation of the two icosahedra-agglomerates situated along [1 1 1], which are so characteristic for β-boron [5, 6]. During the transformation step $\beta' \rightarrow \beta''$, however, some icosahedra have probably left their lattice sites. Whereas the structure factor of the β'-cell allowed only even indices, (1 1 0) appears in the β''-phase in odd and even orders (fig. 4). Possible explanations for this observation may be obtained by structure factor calculations. Assuming that the icosahedra marked "1" and "9" in fig. 11 are pushed from their sites in the β'-cell into positions (x_1, y_1, z_1) and (x_2, y_2, z_2) where

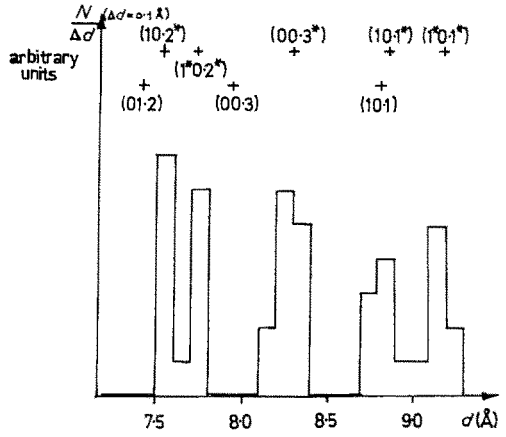

Figure 10 Histogram showing the frequency of experimentally determined lattice spacings related to an interval $\Delta d = 0.1$ Å. Additionally marked are three kinds of d-values.

+ ($hk.l$), d-values of perfect β-boron, indexed with hexagonal cell-data ($a_0 = 10.94$ Å; $c_0 = 23.81$ Å).

+ ($hk.l^*$), d-values assuming a hexagonal unit-cell with $a_0 = 10.94$ Å; $c_0 = 24.90$ Å.

+ ($h^*\,k.l^*$), d-values assuming a pseudo-hexagonal unit-cell with $a_1 = 11.40$ Å; $a_2 = 10.94$ Å; $c_0 = 24.90$ Å.

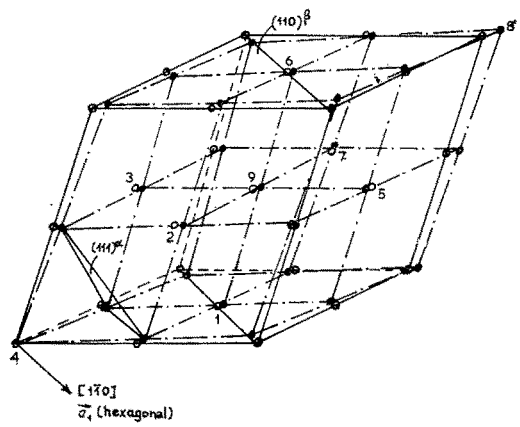

Figure 11 Lattice sites occupied by icosahedra in α-boron (●), after formation of the β'-phase (○).

they compensate mutually their contribution to the structure factor, the observed selection rules will be fulfilled.

When the α-reflections had disappeared at $\approx 1640°$C d-values were found similar to those obtained by shock heating, which were attributed to an anisotropically strained unit cell. Possibly the elongation of the c-axis and one of the hexagonal a-axes is a hint for the beginning arrangement of icosahedra-agglomerates in c-direction. For this purpose all icosahedra, which are not situated on corners and edge middles, must leave their positions and collapse in the interior of the cell. Whether the disappearance of phase boundaries is sufficient or an activation energy for this change of sites is involved in the necessary temperature rise, cannot be decided.

From the fact that it is possible to release the anisotropically strained unit cell by annealing, it can be concluded that an almost correct arrangement of icosahedra-agglomerates is attained by a diffusion-controlled process. Because of the atomic balance, however, the two agglomerates cannot each contain 28 atoms as in the case of perfect β-boron [5, 6]. Looking at fig. 11 it is clear that only icosahedra situated in the centre of a plane can collapse into agglomerates, because corners and edge middles are correct lattice sites in perfect β-boron. From centres of planes $6 \times 12/2 = 36$ boron atoms per unit are available for the formation of agglomerates. These are increased by the 12 atoms of the central icosahedron. So altogether 48 boron atoms are available. On the other hand the unit cell of perfect β-boron contains two agglomerates (each 28 atoms) and an isolated atom in the middle of the cell. This means that 57 atoms are arranged in the "interior" of the perfect β-boron-cell. Consequently the complete elementary cell of β-boron produced by transformation contains 96 atoms compared to 105 of the perfect structure because 48 atoms can be situated on lattice sites of perfect β-boron. Deviations from this perfect cell concerning the icosahedra-agglomerates have previously been reported by Hoard *et al* [5] in β-boron, which was crystallised by rapid cooling from the melt. No irregularities were found in the 84-atomic subunit which can be used to describe the β-boron structure, with the exception of 21 "linking" atoms per unit cell [5]. This subunit, consisting of a central icosahedron and 12 pentagonal pyramids forming the caps of 12 surrounding icosahedra seems to be characteristic for β-boron. This complex can be built up during the transformation when three half-icosahedra from the positions marked 1 (5), 2 (6) and 3 (7) in fig. 11 collapsing into the interior of the cell form three pentagonal pyramids with their quasi five-fold axes parallel to those of the icosahedron at 4 (8). One icosahedron in the centre of the cell (at 9) could bring about the linkage between the truncated icosahedra. The results of this study suggest the

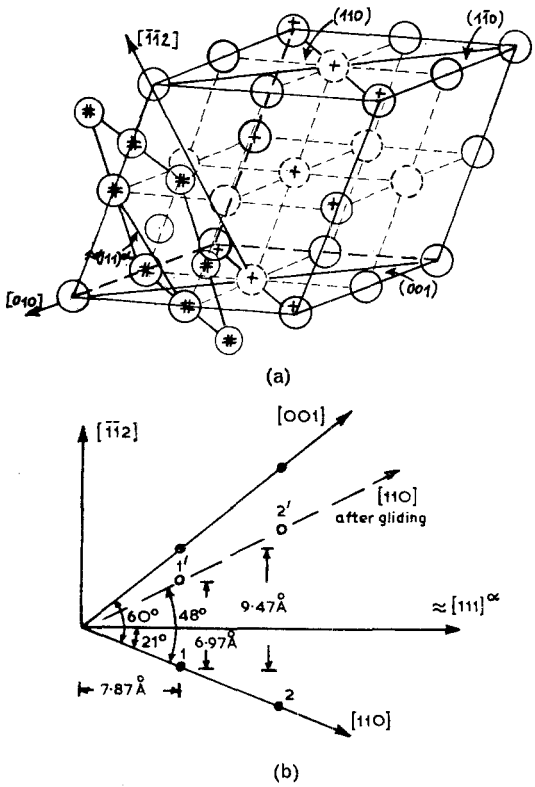

Figure 12 Atomic mechanism producing the observed orientation relationship between α- and β″- boron in two steps (a) first step (b) second step (explanation in the text).

conclusion that the linking of icosahedra-agglomerates can be modified in the β-boron structure.

Knowing the orientation relationship of all transformation products the orientation of the transformed β-boron can be predicted from the orientation of the starting α-boron. However, no unique relationship can be stated between every icosahedron position in the initial lattice and the position it becomes in the final lattice.

Whereas the first and second transformation steps ("expansion" + "rotation") require a co-operative movement of icosahedra maintaining nearest neighbours correlations – and so clearly show martensitic properties – the last step (annealing of the anisotropically strained unit cell) is at least partly diffusion-controlled.

For determination of the habit-plane and for answering the question whether this is an unrotated and either undistorted or isotropically distorted plane, larger crystals of α-boron would be required. Two-surface trace analysis would be possible then, the thinning technique would be easier and so more information from electron micrographs could be obtained.

Acknowledgements

The author wishes to thank Professor Dr J. Jaumann (✠) for suggesting the problem and for his continual interest, Professor Dr H. Alexander for many helpful discussions and valuable advice, Dr W. Dietze for supplying the α-boron and the Stiftung Volkswagenwerk for providing the electron microscope.

Appendix

Estimation of Specimen Temperature

When the condenser II of the electron microscope is defocused a large area is irradiated in the object plane. Consequently the wires of the grid supporting the specimen are heated considerably above the furnace temperature.

In order to estimate the grid temperature two simplifying assumptions were made:

1. The Gaussian intensity profile of the beam current density j_B was approximated by a rectangular profile, the radius of the homogeneously irradiated area being x_0.
2. Heat loss by radiation was neglected in consideration of the high furnace temperature.

The grids were 0.025 mm in thickness, so that the illuminated grid wires absorbed the whole energy of the incident electrons. The density of the thermal energy W_0 produced in the grid wires per second is thus given by:

$$W_0 = \frac{j_B}{e_0} \cdot e_0 \, U_A \cdot \frac{1}{t} \quad (\mathrm{W/cm^3})$$

j_B = beam current density (A/cm²); e_0 = electron charge (A · s); U_A = beam voltage (V); t = thickness of grid wires (cm). This yields:

$$W_0 = 4 \times 10^7 \times j_B \quad (\mathrm{V/cm})$$

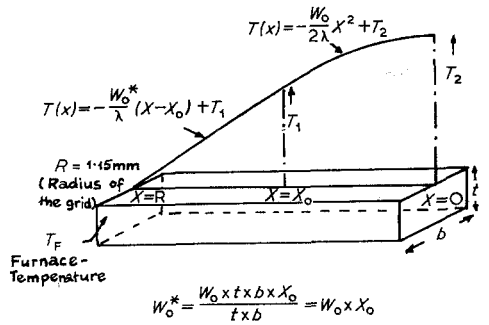

Figure A Approximated temperature distribution in an irradiated grid wire.

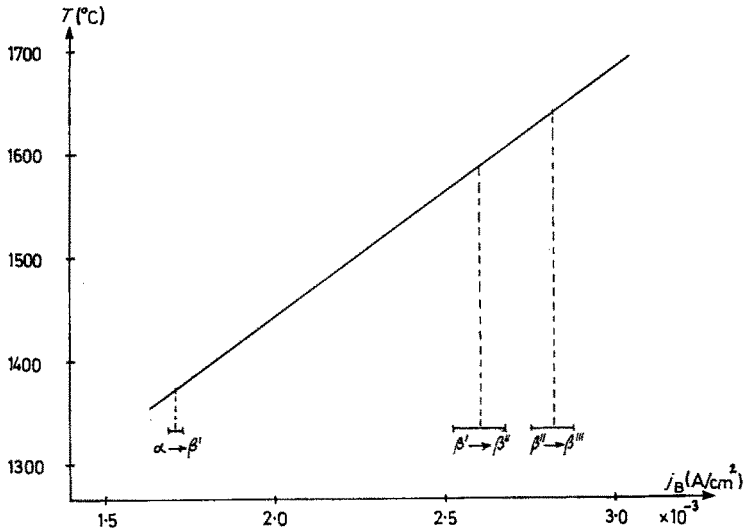

Figure B Approximately calculated specimen temperature using equation 2. Intervals of beam current density are marked in which transformations were observed.

The temperature of the wires of the irradiated area may be approximated by the parabolic temperature distribution in a homogeneously heated rod, a standard problem in thermodynamics. In the un-heated region the temperature falls off linearly due to thermal conduction (see fig. A).

To a first approximation it can be assumed that the temperature distribution is the same in two intersecting wires. The temperature T_2 in the centre of the grid can thus be estimated with the following relation:

$$T_2 = T_F + \frac{W_0 \cdot x_0}{\lambda}(R - x_0) + \frac{W_0}{2\lambda} x_0^2 \; ;$$

$$\lambda_{Mo}(T = 1400\,K) = 0.98 \left(\frac{W}{cm \cdot deg}\right)$$

$$= T_F + 4.08 \times 10^7 \cdot x_0 (R - 1/2\, x_0) \cdot j_B \; (°C/A) \quad \ldots\ldots (2)$$

Near the supporting grid wire the specimen has approximately the temperature of the grid, ideal thermal contact proposed. In self-supporting parts of the specimen, however, at a greater distance from the grid wire the temperature may be markedly higher. The stopping power dE/dz of the specimen material and the thermal conductivity as a function of temperature must then be considered.

The calculations were tested by melting a thin foil of silicon. Melting occurred at a beam current density of $j_B = 1.63 \times 10^{-7}$ (A/cm²), the radius of the illuminated area being $x_0 = 6.4 \times 10^{-2}$ (cm), furnace temperature $T_F = 1000°C$.

Using formula 2 the temperature of the Mo-grid is $T_2 = 1354°C$. In the case of silicon the additional temperature rise in the irradiated specimen can be neglected. The result seems not too bad considering the fact that poor thermal contact between specimen and grid (the silicon foil was pressed with a needle on to the grid) can easily raise the temperature to the melting temperature of silicon (1410°C).

In the case of boron the temperature dependence of the thermal conductivity is not known, so the calculated values can only approximate the temperature of thin boron foils close to supporting grid wires (fig. B).

References

1. J. A. KOHN, W. F. NYE, and G. K. GAULÉ, "Boron I" (Plenum Press, New York, 1960).
2. G. K. GAULÉ, "Boron II" (Plenum Press, New York, 1965).
3. T. NIEMYSKI, "Boron III" (Polish Scientific Publishers, Warsaw, 1970).
4. H. WERHEIT in "Festkörperprobleme X" O. Madelung (Vieweg and Sohn, Braunschweig, 1970) p. 189.
5. J. L. HOARD, R. E. HUGHES, C. H. L. KENNARD, D. B. SULLENGER, H. A. WEAKLIMM, and D. E. SANDS, *J. Amer. Chem. Soc.* **85** (1963) 361.
6. D. GEIST, R. KLOSS, and H. FOLLNER, in "Boron III" p. 109.

7. B. F. DECKER and J. S. KASPER, *Acta Cryst.* **12** (1959) 503.
8. E. AMBERGER and W. DIETZE, *Z. anorg. allg. Chem.* **332** (1964) 131.
9. E. AMBERGER, W. DIETZE, J. JAUMANN, and P. RUNOW, *Phys. Stat. Sol.* a **2** (1970) K 59.
10. W. OSTWALD, *Z. Physikal. Chem.* **22** (1897) 289.
11. LANDOLT-BÖRNSTEIN, "Tabellenwerk, Vol. IV, 2b" (Springer-Verlag, Berlin, 1964).

Received 11 August and accepted 11 November 1971.